

Peptide-Conjugated PAMAM Dendrimer as a Universal DNA Vaccine Platform to Target Antigen-Presenting Cells

Pirouz Daftarian^{1,2}, Angel E. Kaifer⁵, Wei Li⁵, Bonnie B. Blomberg¹, Daniela Frasca¹, Felix Roth¹, Raquibul Chowdhury¹, Eric A. Berg⁷, Jordan B. Fishman⁷, Husain A. Al Sayegh⁶, Pat Blackwelder⁶, Luca Inverardi³, Victor L. Perez², Vance Lemmon⁴, and Paolo Serafini^{1,3}

Abstract

DNA-based vaccines hold promise to outperform conventional antigen-based vaccines by virtue of many unique features. However, DNA vaccines have thus far fallen short of expectations, due in part to poor targeting of professional antigen-presenting cells (APC) and low immunogenicity. In this study, we describe a new platform for effective and selective delivery of DNA to APCs *in vivo* that offers intrinsic immune-enhancing characteristics. This platform is based on conjugation of fifth generation polyamidoamine (G5-PAMAM) dendrimers, a DNA-loading surface, with MHC class II–targeting peptides that can selectively deliver these dendrimers to APCs under conditions that enhance their immune stimulatory potency. DNA conjugated with this platform efficiently transfected murine and human APCs *in vitro*. Subcutaneous administration of DNA-peptide-dendrimer complexes *in vivo* preferentially transfected dendritic cells (DC) in the draining lymph nodes, promoted generation of high affinity T cells, and elicited rejection of established tumors. Taken together, our findings show how PAMAM dendrimer complexes can be used for high transfection efficiency and effective targeting of APCs *in vivo*, conferring properties essential to generate effective DNA vaccines. *Cancer Res*; 71(24); 7452–62. ©2011 AACR.

Introduction

The use of naked plasmid DNA as a vaccine to prime the immune system provides a variety of practical benefits for large-scale production that are not as easily achievable with other forms of vaccines including recombinant proteins or whole tumor cells (1–4). While numerous clinical trials have proven the safety of this cost effective vaccination strategy, they have also revealed its limitations, as the

immune response elicited is insufficient to clear established tumors or infections. The low *in vivo* transfection efficiency, the absence of preferential targeting of professional antigen-presenting cells (APC), and the modest intrinsic adjuvant activity of DNA vaccines are thought to be the main reasons for the marginal effect observed in clinical studies and in therapeutic murine models. An accepted assumption is that the immunogenic potency of DNA-based vaccines can be significantly increased if the delivery of DNA to professional APCs is maximized and if additional immunologic help in the form of adjuvants and/or cytokines is provided (5, 6).

We present here a new platform for DNA delivery that fulfills these characteristics. This platform is based on the use of generation 5 polyamidoamine (G5-PAMAM) dendrimers conjugated with MHC class II–targeting peptides.

Although PAMAM dendrimers have been tried as vaccine platform as their positive charge allows the complexation at physiologic pH of DNA protecting it from nuclease and increasing the transfection efficiency (7, 8), *in vivo*, they showed only modest success. A marginally significant increase in vaccine efficacy was obtained also with universal peptides used as adjuvant, although a large number of helper T cells were activated by these molecules (9). In contrast, the conjugation of PAMAM dendrimer and universal peptides not only combines their positive properties but allows a highly selective delivery of DNA to APCs which dramatically increases the efficacy of DNA vaccines (Supplementary Fig. S1).

Authors' Affiliations: ¹Department of Microbiology and Immunology, Sylvester Cancer Center, ²Bascom-Palmer Eye Institute, ³Diabetes Research Institute, and ⁴Miami Project to Cure Paralysis, Department of Neurological Surgery, Miller School of Medicine, University of Miami, Miami; ⁵Center for Supramolecular Science and Department of Chemistry, and ⁶University of Miami Center for Advanced Microscopy (UMCAM), University of Miami, Coral Gables, Florida; and ⁷21st Century Biochemicals, Inc., Marlborough, Massachusetts

Note: Supplementary data for this article are available at Cancer Research Online (<http://cancerres.aacrjournals.org/>).

P. Daftarian and P. Serafini contributed equally to this work.

Corresponding Authors: Paolo Serafini, Department of Microbiology & Immunology, University of Miami, 1600 NW 10th avenue, 3075 RMSB Bldg (R138), Miami, FL 33136. Phone: 305-243-7917; Fax: 1-305-243-5522; E-mail: pserafini@med.miami.edu; and Pirouz Daftarian, Departments of Microbiology & Immunology and Ophthalmology, 608 McKnight-Vision Research, 1638 NW 10th avenue, Miami, FL 33136. Phone: 305-243-7919; E-mail: pdaftarian@med.miami.edu

doi: 10.1158/0008-5472.CAN-11-1766

©2011 American Association for Cancer Research.

Materials and Methods

Cell lines and culturing conditions

B16F10 (ATTC) is a C57BL/6 melanoma cell line. B16 melanoma cells (H2^b) stably expressing chicken OVA (B16OVA.pc) were provided by Dr. G. Barber (University of Miami, Miami, FL). MBL2, a lymphoma cell line derived from C57BL/6 mice; CT26, a BALB/c-derived colon carcinoma; and TSA, a BALB/c-derived mammary tumor adenocarcinoma were kindly supplied by Dr. V. Bronte (University of Verona, Verona, Italy). Cell lines were cultured in complete medium [RPMI-1640 media (Invitrogen) supplemented with 2 mmol/L L-glutamine, 10 mmol/L HEPES, 20 μmol/L 2-mercaptoethanol, 150 μg/mL streptomycin, 200 μg/mL penicillin, and 10% heat-inactivated FBS (Invitrogen)]. B cells from ficolled peripheral blood mononuclear cells (PBMC) were isolated by negative selection using anti-biotin microbeads (Miltenyi Biotech) after staining with a biotinylated anti-CD3 antibody (BD Biosciences), according to the MiniMacs protocol (Miltenyi Biotech). After purification, B cells (10⁶ per mL) were cultured overnight in complete medium supplemented with 5 μg/mL CpG (ODN 2006; Invivogen). Human dendritic cells (DC) were differentiated from monocytes isolated from ficolled PBMCs with granulocyte-macrophage colony-stimulating factor (GM-CSF; 10 ng/mL) and interleukin 4 (IL-4; 10 ng/mL) for 5 days. Maturation was induced by adding the mimic maturation cocktail [TNFα (5 ng/mL), IL-1β (5 ng/mL), IL-6 (75 ng/mL), and prostaglandin E2 (PGE2; 1 μg/mL)]. Experiments were carried out using PBMCs isolated from healthy adult volunteers after appropriate signed consent and Institutional Review Board approval.

ELISA

Mixed lymphocyte peptide cultures (MLPC) were carried out by culturing 25 × 10⁶ red blood cells (RBC)-lysed splenocytes with 10 mL of 1 μmol/L peptide for 5 days at 37°C 5% CO₂ in a 25 mL flask (BD Biosciences). A total of 10⁵ MLPCs derived T cells were restimulated for 24 hours with an equal amount of target cells; the supernatants were harvested and tested for the IFN-γ released in a sandwich ELISA (Endogen) following manufacturer's instructions.

Flow cytometry

The detailed protocol for cell staining and the list of the antibodies used is described in the Supplementary Material.

Fluorophore-linked immunosorbent assay (FLISA) was conducted as previously described (10) and further described in the Supplementary Material.

Peptides and plasmids

pcDNA3 (Invitrogen), pcDNA3-tyrosine-related protein-2 (TRP2) and pcDNA3-gp70 were previously described (11, 12). pcDNA3-ovalbumin (pcDNA3-OVA) was a gift from Dr. Barber (University of Miami, Miami, FL) and pMAX-GFP were obtained from Lonza. All plasmids were prepared by the endotoxin-free Gigaprep Kit (Invitrogen). The following peptides were used: gp70-derived AH1, SPSYVYHQF (AnaSpec); TRP2₁₈₀₋₁₈₈, SVYDFVWL (AnaSpec); PAN DR epitope

(PADRE), aKXVAAWTLKAAaZC (21st Century Biochemicals, Inc.); and modified HemoAgglutinin HA₁₁₀₋₁₂₀, SFERFEIFP-KEC (HA; 21st Century Biochemicals, Inc.).

Conjugation of the peptides to the dendrimers

Peptide-dendrimer conjugates were manufactured by crosslinking 5th generation dendrimer (Dendritech) and peptides target as follows: PADRE and HA₁₁₀₋₁₂₀ with an added cysteine at the c-terminus with maleimido-*bis*-succinimidyl ester (MBS; Sigma-Aldrich) as reported in the Supplementary Material.

DNA-nanoparticle complexation

DNA (100 μg/mL) was resuspended in warm (37°C) PBS (pH 7.4; Invitrogen) for scanning electron microscopy (SEM) and ethidium bromide (EtBr) exclusion assay or Opti-MEM (Invitrogen) for DNA vaccine and *in vitro* transfection. DNA solution was added drop wise to the nanoparticles with a p100 tip to an equal volume of DNA versus nanoparticles while the vial containing nanoparticle was being vortexed. Amine:phosphate (N:P) ratio 10:1 was used unless otherwise indicated.

EtBr exclusion assay

A total of 100 μL of DNA (50 μg/mL) were admixed in a 96-well plate with different amounts of nanoparticle and incubated for 5 minutes at room temperature. EtBr was added (400 ng/mL), fluorescence determined on a VERSA doc 3000 (Biorad) and images analyzed by ImageJ (<http://rsbweb.nih.gov/ij/>). Data from duplicate wells are reported as percentage of free DNA using the formula: %_{free DNA} = (FI)^{experimental} / (FI)^{control} × 100.

Mice and vaccination

Eight-week-old C57BL/6 (H2^b) and BALB/c (H2^d) mice were purchased from Harlan. Procedures involving animals and their care conformed to institutional guidelines that comply with national and international laws and policies and were approved by the University of Miami IACUC. In experiments with tumors, mice were ear tagged, randomized after treatment, and tumor growth was monitored 3 times a week with a caliper by an investigator blinded to the treatment. Mice were euthanized when the tumor size index (the product of 2 perpendicular diameters) was bigger than 100 mm². Vaccination with the DNA-nanoparticle complexes was carried out by subcutaneous injection of 200 μL of DNA-nanoparticle complexes at an N:P ratio = 10:1 in Opti-MEM (Invitrogen). Dermal electroporation (13) was carried out with DermaVax (Collectis-Bioscience Inc.) following manufacturer's instruction and further detailed in the Supplementary Methods.

Statistical analysis

SigmaPlot (Systat Software Inc.) was used for statistical analysis. One-way ANOVA was conducted after normality evaluation by Kolmogorov-Smirnov test. Pairwise posthoc analysis was conducted using the Holm-Sidak test or the Dunn test. ANOVA on ranks was used if the sample were not normally distributed. The Student *t* test was used when 2 groups needed

to be compared. Kaplan–Meier log-rank followed by the Holm–Sidak posthoc analysis was used to evaluate the survival differences between groups.

SEM

B cells were fixed (24 hours in 4% glutaraldehyde in 0.1 mol/L PBS buffer at 4°C), rinsed 3 times in PBS, and postfixed in 1% osmium tetroxide for 20 minutes. Cells were dehydrated in a graded series of ethanol, rinsed with hexamethyldisilazane, placed on bare aluminium stubs (12-mm diameter), and outgassed overnight. The samples were sputter coated with palladium in a Cressington-108 Auto Sputter Coater and imaged in a Phillips XL-30/ESEM-FEG (15–30 kV).

Results

Synthesis and characterization of peptide-conjugated PAMAM dendrimer

To target the dendrimer to the APCs, we used the following 2 MHC class II–restricted peptides: (i) the influenza hemoagglutinin-derived H2-I-E^d–restricted HA_{110–120} peptide and (ii) PADRE which has high affinity for more than 95% of all human leukocyte antigen-D related (HLA-DR) and for the murine H2-I-A^b (9, 14–16). Considering that many dendrimers would bind to a single DNA molecule, we hypothesized that the conjugation of 2 to 3 peptides to a dendrimer could ensure the proper targeting to MHC class II while leaving 125 to 126 amine groups

available for DNA binding. Peptide–dendrimer conjugates were manufactured by crosslinking G5-PAMAM dendrimer [average molecular weight (MW): 28,826 Da] to either PADRE (MW: 1,611 Da) or HA_{110–120} with an added cysteine at the c-terminus (MW: 1,573 Da) via MBS. Pilot experiments (Supplementary Fig. S2) determined that 8 mol/L excess concentrations of MBS for derivatizing the dendrimers followed by a 4 mol/L excess of purified peptide were the optimal conditions as determined by reversed-phase high-pressure liquid chromatography (RP-HPLC) and mass spectrometry (Supplementary Fig. S3).

Reaction products [PADRE-conjugated PAMAM Dendrimer (PPD) and HA-conjugated PAMAM Dendrimer (HAPD)] were purified by HPLC (Supplementary Fig. S3A and S3B) resulting in an essentially pure material with negligible contamination by either free dendrimer or peptides.

Effective conjugation of the peptide to the dendrimer was indicated by proton nuclear magnetic resonance (¹H-NMR) spectroscopy (Fig. 1A) and confirmed by UV-visible spectroscopy (Fig. 1B and Supplementary Fig. 3C). The average mass of the purified peptide-nanoparticle (Fig. 1C) was 32,060 Da, consistent with a G5-PAMAM dendrimer conjugated with approximately 2 PADRE peptides.

The positive charges of dendrimer are important for strong electrostatic interactions with negatively charged DNA to form the final complexes that are delivered to

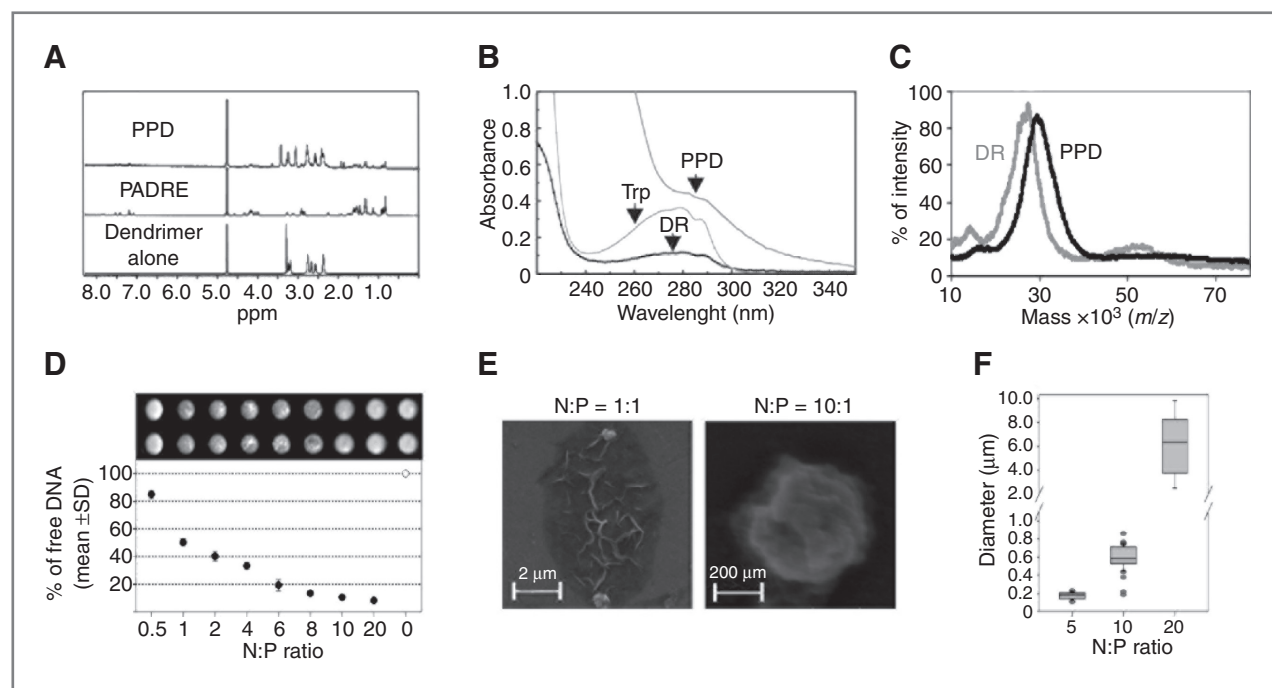


Figure 1. Construction and characterization of peptide dendrimer. A, ¹H-NMR spectra of Dendrimer (DR) alone, PADRE peptide alone, and PPD in D₂O showing that PADRE peptides are connected to the dendrimer. B, UV spectral analysis of PPD, tryptophan (Trp), unconjugated dendrimer or PPD. C, matrix-assisted laser desorption/ionization–time-of-flight (MALDI-TOF) mass spectrometry showing PPD (black line) or unmodified DR (gray line). D, EtBr exclusion assay: 5 μg of DNA were mixed with PPD as described in Materials and Methods and the (E) SEM photograph of PPD complexed with pMAX-GFP at 1:1 or 10:1 N:P ratio. F, the size of complexes (*n* = 40) formed at different N:P ratio was analyzed with ImageJ. Median, 10th, 25th, 75th, and 90th percentile as well as the outlier are indicated.

the target cells; however, the size and biological properties of the DNA–nanoparticle complexes are dependent on the ratio between the positively charged amine (N) in the dendrimer and the negatively charged phosphate (P) in the DNA. EtBr exclusion assay (Fig. 1D) determined that at an N:P ratio of 10:1 more than 90% of the DNA was complexed with the dendrimer. No macroscopic precipitates were visible at 40 \times magnification with optical microscopy (data not shown). DNA-peptide-dendrimer complexes generated at different N:P ratios were further characterized by SEM. At a 1:1 N:P ratio the formation of filament-shaped particles (Fig. 1E) suggested incomplete complex formation. Globular particles with a diameter of approximately 200 and 600 nm were generated when 5:1 and 10:1 ratios were used. At higher N:P ratios, macroprecipitates were generated (Fig. 1F and Supplementary Fig. S4). These data indicate that it is possible to conjugate peptides to the dendrimers without affecting their capacity to bind and complex DNA. However, we observed that variations of the N:P ratio resulted in the generation of complexes of different sizes and shapes, highlighting that this is an important variable that must be accounted for when analyzing the outcomes of the transfection experiments.

Dendrimers conjugated with MHC class II-binding peptides preferentially target APCs *in vitro* and *in vivo*

To verify whether PPD or HAPD are efficient in targeting APCs and determine the N:P ratio with the optimal transfection efficiency, pMAX-GFP was complexed with the PPD nanoparticle or with unconjugated dendrimers at different N:P ratios and used to transfect magnetically purified human B cells (Fig. 2A and B) or monocytic-derived human DC (Fig. 2C). fluorescence-activated cell-sorting (FACS) analysis conducted 48 hours after transfection with PPD-GFP revealed that GFP expression was maximal at a 10:1 N:P ratio (Fig. 2A) by either mean fluorescence intensity (MFI) or percentage of transfected cells (Fig. 2B), whereas the transfection efficiency of the unconjugated dendrimer was inferior at the same N:P ratio. Similar data were obtained using PPD on C57BL/6 splenocytes or HAPD-GFP on BALB/c splenocytes (data not shown) or when human DCs were used (Fig. 2C), suggesting that, while complex size can play an important role in PPD ability to transfect the target cells, it minimally influences its specificity. Interestingly, PPD-mediated transfection of immature DC induced the upregulation of CD40, but not CD80, even in the absence of maturation cocktail (mimic, Fig. 2D). To further evaluate the specificity of the DNA–PPD complexes,

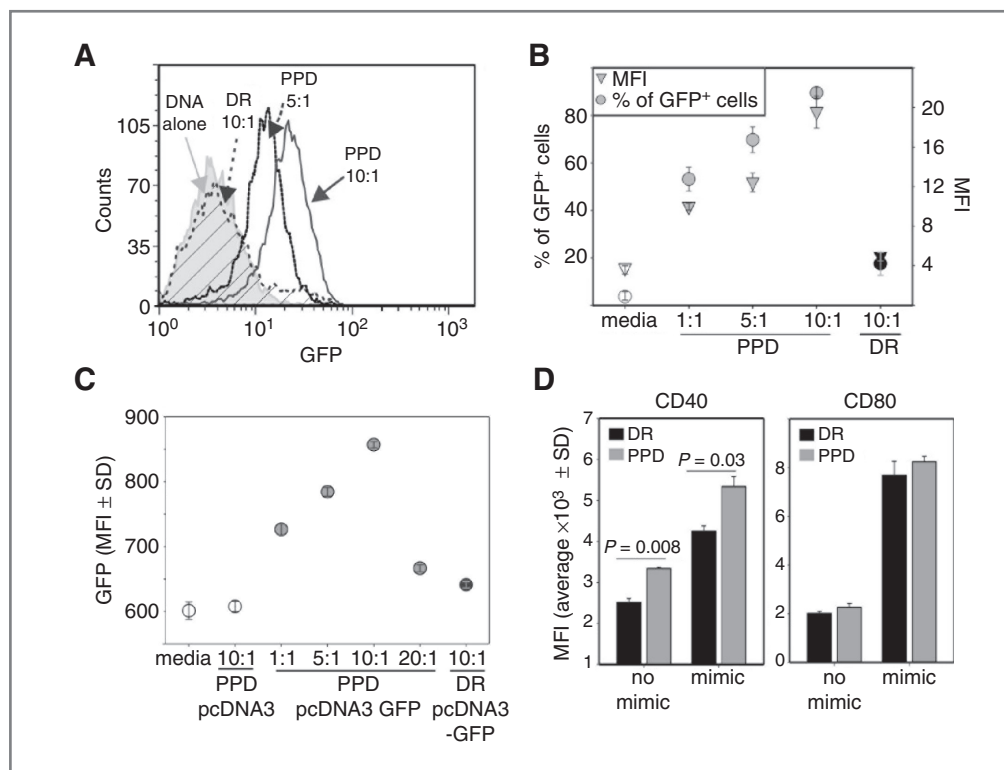


Figure 2. PPD and HAPD transfect efficiently APCs *in vitro*. A, A total of 10⁵ magnetically purified human B cells were incubated for 20 minutes with 5 μ g pMAX-GFP complex at the indicated ratio with PPD or unconjugated dendrimer. After 48 hours, GFP fluorescence was evaluated by FACS. Data from duplicate samples are summarized in (B) where percentage of GFP-positive cells (circle) and GFP MFI (triangle) are reported for PPD (gray symbol), unconjugated dendrimer (in black), or untransfected cells (in white). C, human DC were differentiated from monocytes precursors using GM-CSF and IL-4 for 5 days and GFP transfected using PPD or dendrimer at the indicated N:P ratio. Maturation cocktail (mimic) was added 2 hours after the transfection, and GFP intensity was evaluated 24 hours later. D, immature human DC prepared as in (C) were transfected with pcDNA. Maturation cocktail (mimic) was added where indicated, and expression of CD40 and CD80 was evaluated 24 hours later.

unconjugated dendrimer or PPD loaded with pcDNA3 were incubated for 20 minutes at room temperature with magnetically purified human B cells. Cells were then washed, fixed, and imaged in the SEM (Supplementary Fig. S1B). Whereas particles with a size similar to the DNA-PPD complexes were found on the membrane of B cells treated with PPD (Supplementary Fig. S1B), similar structures were undetectable in the B cells treated with unconjugated dendrimer. These data indicate that N:P ratio = 10:1 results in maximum transfection and that the addition of MHC class II-binding peptide increases the *in vitro* transfection efficiency of the dendrimer in APCs.

To evaluate the efficiency and specificity of these platforms *in vivo*, PPD or HAPD dendrimers complexed with pMAX-GFP (PPD-GFP and HAPD-GFP) were injected subcutaneously into C57BL/6 or BALB/c mice, and draining lymph nodes were harvested and analyzed 48 hours later. Controls included mice injected with PBS or with a pMAX-GFP-loaded unconjugated dendrimer. Whereas only basal fluorescence was found in the contralateral lymph nodes, FACS analysis revealed a higher number of GFP⁺, MHC class II⁺ cells in the draining lymph node of mice treated with PPD (Fig. 3A), indicating a preferential *in vivo* targeting of APCs. These GFP⁺ cells were mostly mature DC as revealed by the expression of H2-I-A^b, CD11c,

CD80, and CD86 (Fig. 3B). A total of 50% of the transfected DC were CD11b^{high}CD103^{low/neg}CD8^{low/neg}, 30% CD11b^{low}CD8^{low/neg}CD103^{low/neg} DC, the remaining were CD11b^{low} and positive for CD8 and/or CD103 (Fig. 3B). Similar ratios were found in the untransfected DC from the contralateral lymph node, suggesting the absence of a preferential targeting for any of the examined DC subsets. Interestingly, the absolute number of DC was also elevated (Fig. 3C and D) in the PPD group, confirming the immunostimulatory properties of this peptide (14). Conversely, mice treated with unconjugated dendrimer showed only marginal GFP fluorescence increase in the draining lymph nodes (Fig. 3A) and fewer GFP⁺ DC (Fig. 3C). Results similar to those seen with PADRE were obtained using the HAPD platform in BALB/c mice (Fig. 3D).

While PPD or HAPD should target all the MHC class II-positive cells, only a limited number of transfected B cells are found in the draining lymph nodes (data not shown). At present, we cannot discriminate whether this is due to preferential targeting of DC or if transfected B cells have different homing properties.

These data indicate that PPD and HAPD are superior, when compared with unconjugated dendrimers, for promoting the

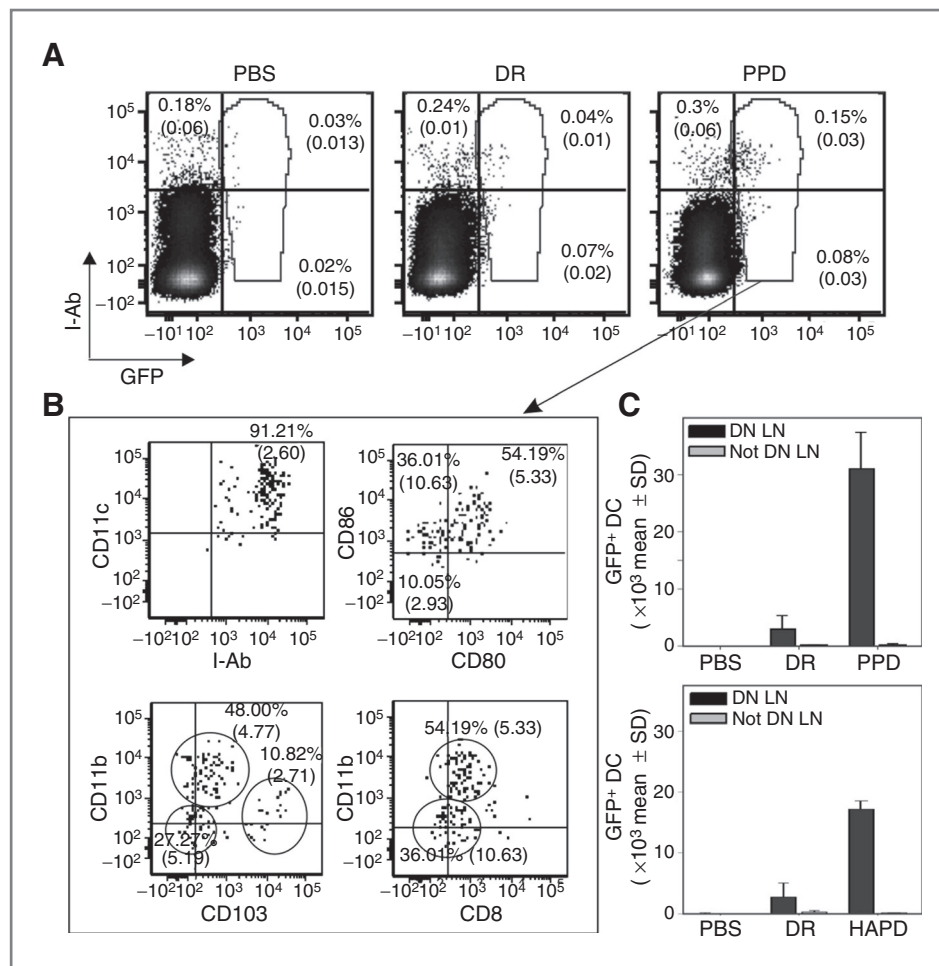


Figure 3. PPD and HAPD transfect preferentially DC *in vivo*. A, PBS, unconjugated dendrimer, or PPD loaded with pMAX-GFP were injected subcutaneously in the right flank of C57BL/6 mice. After 4 days, draining lymph nodes were harvested, cells labeled with the indicated antibodies and a vital dye, and analyzed by FACS for the expression of GFP. Representative dot plots of the live cells are shown. GFP⁺ cells as gated in (A) were further analyzed (B) using the indicated antibodies. C, the number of GFP⁺CD11c^{high}I-Ab^{high}DC present in the draining lymph node (DN LN) of C57BL/6 mice vaccinated as described in (A) is reported. D, the same experiment was repeated in BALB/c mice vaccinated with HAPD, unconjugated dendrimer (DR), or PBS. Data are expressed as the number of GFP⁺ DC recovered in the lymph nodes from one experiment (3 mice/group) and are representative of other 3 independent experiments.

transfection of APCs *in vitro*; more importantly *in vivo* they are clearly capable of preferentially transfecting professional APCs most of which seem to be DCs.

PPD and HAPD promote generation of high affinity T cells and induce a powerful humoral response

To determine whether the higher transfection specificity of the PPD platform *in vivo* results in effective immunization in mice, we used the weak, self-melanocyte differentiation antigen TRP2. TRP2 is the main antigenic target of the immune response elicited in mice by immunization with genetically modified B16 melanoma vaccines (17, 18). The anti-TRP2 immune response is dominated by CD8⁺ T cells that can either have high avidity and elicit protection upon B16 challenge or have low avidity and fail to protect (18). Whereas both high and low avidity clones can recognize TRP2 pulsed on MBL2 cell line, only high avidity clones can recognize unpulsed B16 cells (18). C57BL/6 mice were immunized with pcDNA3-TRP2 or pcDNA3 using PPD or unconjugated dendrimers. Seven days later, mice were sacrificed and splenocytes stimulated with the relevant or irrelevant peptide. The cultures were then harvested, washed, and cultured for 24 hours with B16 cells or with MBL2 cells pulsed with TRP2 or with an irrelevant peptide. IFN- γ ELISA was used as read out for CTLs activation. T cells isolated from mice immunized with either dendrimer-TRP2 or PPD-TRP2 can recognize TRP2-pulsed MBL2 (Fig. 4A); however, IFN- γ secretion from the PPD group is 10 times higher than that seen with the control dendrimer. Conversely, only T cells from the group immunized with PPD-TRP2 recognize the antigen endogenously expressed by the B16 melanoma. Moreover, memory CTLs can be generated by the PPD platform as revealed by the experiments shown in Fig. 4B, in which the immune response in mice vaccinated twice (at day 0 and 7) with PPD-TRP2 or DR-TRP2 was measured at day 40. These data suggest that the conjugation of PADRE peptide to dendrimers enhances the immune response obtained by the dendrimer, generating high affinity memory T cells capable of recognizing not only TRP2-pulsed MBL2 but also the rare MHC class I molecules endogenously loaded with TRP2 in the B16 melanoma (12). Similar data were obtained when HAPD was used in conjunction with the natural occurring tumor-associated gp70 antigen derived from the envelope protein of a murine endogenous retrovirus (19); whereas T cells from both HAPD-gp70 and DR-gp70 can recognize APCs pulsed with the immunodominant gp70-derived AH1 peptide, only T cells from mice vaccinated with the HAPD particle were able to recognize the gp70⁺ CT26 tumor (Fig. 4C).

Peptide-conjugated dendrimers not only generate high affinity CTLs but also a humoral response. FLISA analysis (Fig. 4D) reveals that a single vaccination with pcDNA3-OVA results in high anti-OVA antibody titers in all vaccinated mice when PPD is used, whereas only modest results were obtained when unconjugated dendrimers or when dermal electroporation were used (Fig. 4D). Similar results were obtained using 3 additional antigens in conjunction with PPD (data not shown). When electroporation or HAPD were used to vaccinate BALB/c mice using pcDNA3 encoding the viral G protein-coupled receptor (vGPCR), inferior results were obtained even when

vaccination was conducted twice (Fig. 4E); whereas electroporation generated high antibody titer in all mice analyzed, HAPD led to the generation of a good humoral response only in 4 of 8 of the mice (Fig. 4E). These data indicate the capacity of PPD and HAPD to generate a humoral response and the generation of high affinity memory CTL with high affinity for the relevant antigen.

PPD is more effective than electroporation in promoting antitumor immunity

To compare the immunity induced by the PPD and HAPD platforms to that induced by dermal electroporation, today's gold standard for DNA vaccination, we used 2 tumor mouse models (B16OVA and CT26) in which electroporation has been shown to result in long-term survival of approximately 30% to 40% of the vaccinated mice (Fig. 5). Whereas all mice vaccinated with pcDNA3 developed and succumb to the B16OVA tumor by day 28, prophylactic electroporation with pcDNA3-OVA resulted in a significant reduction of tumor appearance and growth, with a 20% survival rate of the mice. When OVA immunization was carried out with PPD, approximately 75% of the mice exhibited no tumor growth, showing a better therapeutic efficacy than the one obtained with electroporation ($P = 0.001$, Fig. 5A). Different results were obtained in the CT26 model using HAPD to immunize BALB/c against gp70. Whereas prophylactic electroporation with pcDNA3-gp70 resulted in the survival of 40% of mice challenged with CT26, gp70 immunization with HAPD allowed only 10% of the animals to survive, even if the delay in tumor formation seen in the group vaccinated with gp70 reached statistical significance (Fig. 5B). Indeed, while electroporation and PADRE peptide should provide a "danger signal" that can promote the generation of strong immunity (14, 20), this may not occur when the HA helper peptide, a nonuniversal T helper epitope, is used (21). In additional experiments, in which we tested the immunogenicity of PPD in an immune-privileged site such the eye (22), a single intracorneal immunization with 2 μ g of PPD-GFP was sufficient to induce an elevated anti-GFP humoral response (Supplementary Fig. S5). No anti-GFP antibodies were detected when unmodified dendrimers were used, further elucidating the strong adjuvant effect associated with the use of PPD.

PPD-mediated TRP2 vaccination leads to the rejection of established melanoma

If targeting DNA vaccine to MHC class II⁺ APC is important in a prevention setting, in a therapeutic model where tolerogenic mechanisms are elicited and the tumor is established, delivering the antigen to the professional APC might become the key for successful therapy (23). PPD nanoparticles were therefore tested in the stringent therapeutic murine tumor melanoma model B16 (Fig. 6). As mentioned earlier, the B16 tumor-associated antigen TRP2 is a weak antigen and only modest results are obtained when TRP2 is used to treat established melanomas (24) unless the antigen vaccination is carried out using powerful recombinant vaccinia virus (18) or combinatorial treatment (24, 25). Coherent with previous results, immunization against TRP2, conducted 2 and 9 days after tumor injection using peptide unconjugated, control

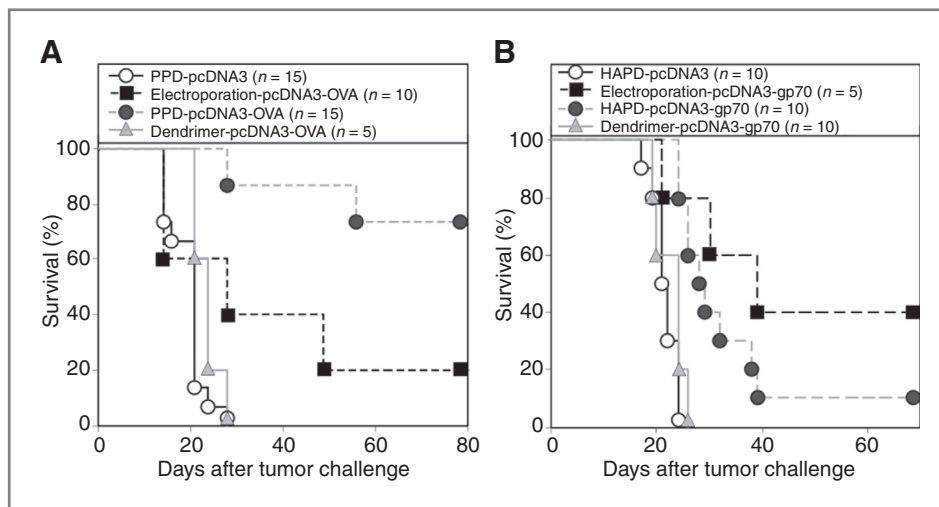
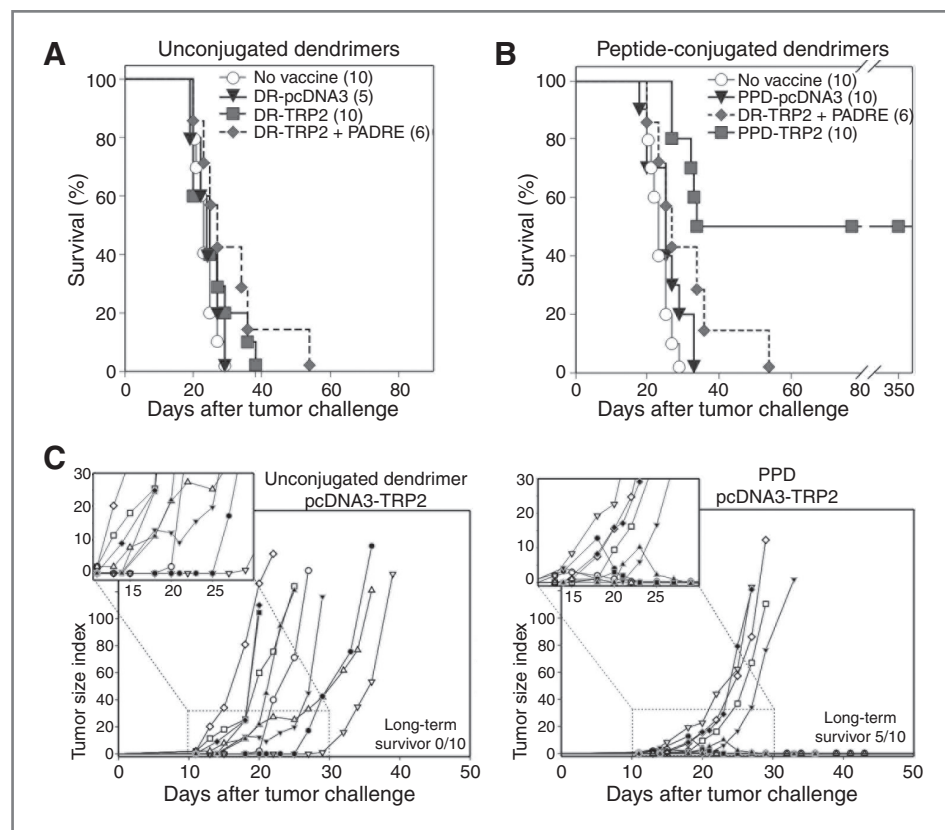


Figure 5. A, A total of 5×10^4 B16OVA cells were injected on day 0 in C57BL/6 mice previously vaccinated (at day -10 and -25 days) with 20 μ g of pcDNA3-OVA. Immunizations were conducted using electroporation (black square), or by subcutaneous injection of PPD particle (dotted gray circle), or unmodified dendrimer (gray triangle). As control, an additional group of mice was vaccinated using PPD loaded with pcDNA3 (black circle). Data are derived from 3 independent experiments. Log-rank $P < 0.001$, Holm-Sidak: PPD-OVA versus PPD-pcDNA3 or DR-OVA $P < 0.00001$; PPD-OVA versus EP $P < 0.001$; EP versus PPD-pcDNA3 $P = 0.02$. B, BALB/c mice, vaccinated at day -15 and -8 with pcDNA3gp70 (20 μ g), were challenged with 5×10^4 CT26 cells at day 0. Immunization was conducted using dermal electroporation (black square), HAPD nanoparticle (gray-dotted circle), or control DR (gray triangle) subcutaneously. As an additional control, a group of mice was vaccinated with HAPD loaded with pcDNA3 (black circle). Data are derived from 2 independent experiments. Log-rank $P < 0.001$, Holm-Sidak: HAPD-gp70 versus HAPD-pcDNA3 $P < 0.001$; EP versus HAPD-pcDNA3 $P < 0.001$.

gp70 immunizations on days 2 and 9 post-TSA injection did not increase mice survival, the use of either HA peptide admixed to the vaccine or HAPD showed statistically significant, albeit modest, survival advantages (HAPD-

pcDNA3gp70 vs. HAPD-pcDNA3 $P < 0.01$; Fig. 7A). Because TSA is an extremely immunosuppressive tumor, in which regulatory T cells (T_{reg}) may play an important role (ref. 28; and Roth, Serafini unpublished data), we wanted to

Figure 6. PPD promotes the rejection of established B16 melanoma tumors. C57BL/6 mice were injected subcutaneously on the right flank with the B16F10 tumor on day 0. On day 2 and 9, mice received as vaccine pcDNA3-TRP2 (gray square) or pcDNA3 (as control, black triangle) subcutaneously distributed in 4 anatomic sites (10 μ g/site). Immunization was conducted using either unmodified DR (A) or PPD with (B). As additional controls, mice received PBS (white circle) or unmodified dendrimer loaded with pcDNA3-TRP2 and mixed with the same dose of PADRE peptide theoretically linked to the PPD (DR-TRP2 + PADRE; gray diamond). Log-rank $P < 0.001$, Holm-Sidak: PPD-TRP2 versus PPD-pcDNA3, $P = 0.001$; PPD-TRP2 versus DR-TRP2 + PADRE, $P = 0.03$; DR-TRP2 + PADRE versus no vaccine, $P = 0.04$. C, tumor growth for the DR-TRP2 or the PPD-TRP2 group.



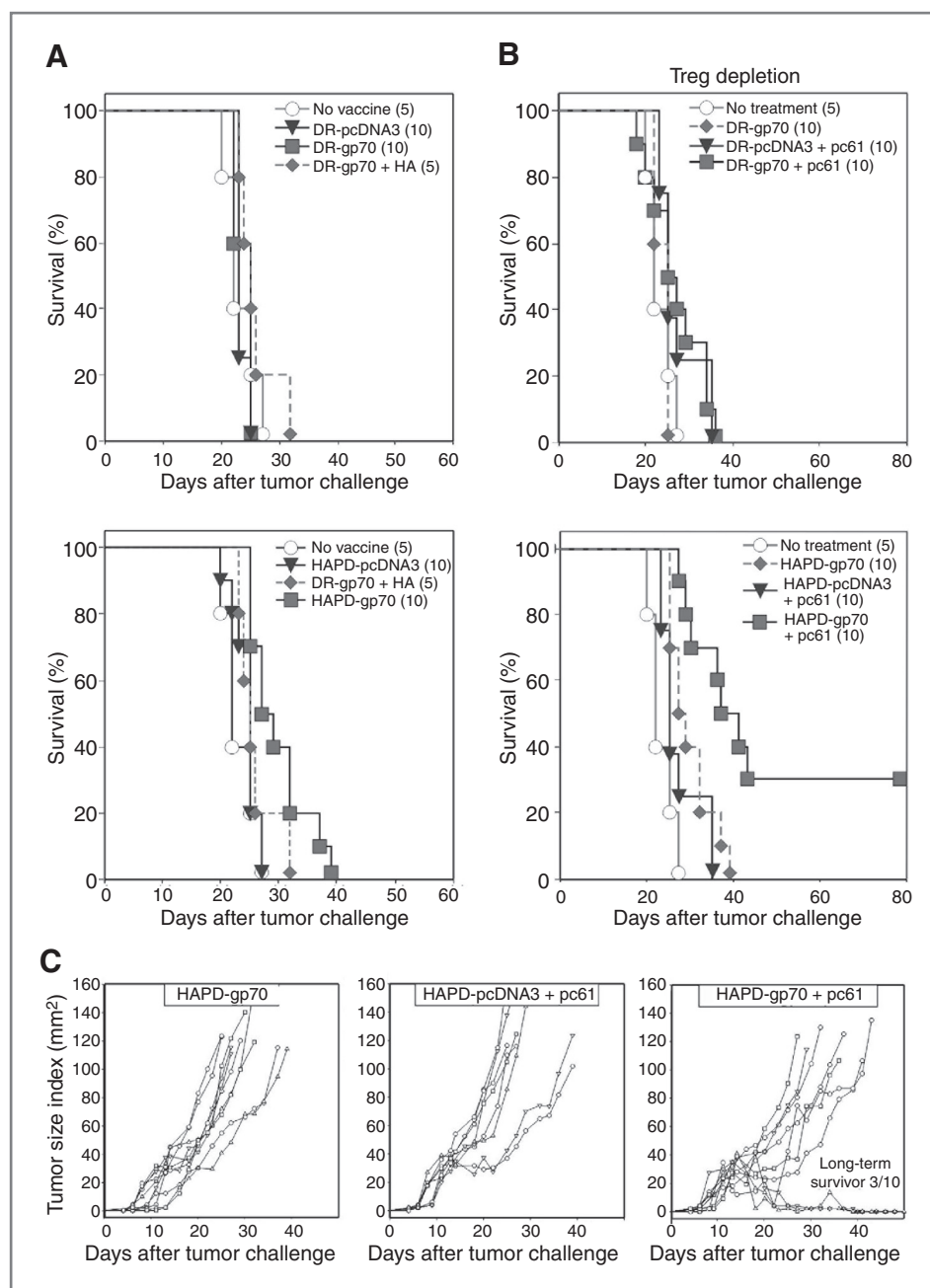


Figure 7. T_{reg} depletion enhances the therapeutic efficacy of HA-mediated gp70 vaccination in the TSA mammary carcinoma model. BALB/c mice injected with 5×10^4 TSA cells on day 0 received, on day 1 and 7, 40 μ g of pcDNA3-GP70 subcutaneously divided in 4 different sites. Immunization was conducted using unmodified dendrimer (DR-gp70, gray square, top) or HAPD (HAPD-gp70, gray square, bottom). As control, mice received pcDNA3 (black triangle) or PBS (white circle). An additional group of mice receive a mixture of DR-gp70 and HA peptide (gray diamond). Log-rank $P = 0.011$, Holm-Sidak: HAPD-gp70 versus HAPD-pcDNA3, $P < 0.001$. B, half of the mice in each group were intraperitoneally injected with isotype control (A) or with the anti-CD25 depleting antibody PC61 (100 μ g) on day -1, 5, 12, and 21 (B). Untreated and unvaccinated mice were used as an additional control (white circle). Log-rank $P < 0.001$, Holm-Sidak: HAPD-gp70 versus HAPD-pcDNA3 + pc61, $P < 0.001$; HAPD-gp70 versus HAPD-gp70 + pc61, $P = 0.007$. C, tumor growth for the HAPD-gp70, pc61 group, or the combined treatment.

determine whether T_{reg} depletion could enhance the therapeutic efficacy of HAPD-gp70. As shown in Fig. 7 (top) anti-gp70 vaccination using unmodified dendrimers did not increase the survival of the mice compared with the control when PC61 (the anti-CD25 depleting antibody) is administered. Conversely, PC61 treatment restored the therapeutic efficacy in mice vaccinated with HAPD-loaded pcDNA3-gp70, prolonging the median survival time (MST) of almost 70% ($MST_{HAPD-gp70} = 37$ days; $MST_{no\ treatment} = 22$ days) and resulting in 30% mice survival. Although the adjuvant effect of pc61 treatment in the TSA model has not yet been characterized, these results suggest the efficacy of

our platform can be further increased by a multifaceted approach that includes targeting of suppressor cells.

Discussion

Although early data from clinical trials with DNA vaccines delivered by *in vivo* electroporation which greatly enhances the *in vivo* transfection efficiency are cautiously promising (29), it is thought that the real promise of DNA vaccines can only be fulfilled when efficient *in vivo* targeting of professional APCs is combined with the proper adjuvant (5).

Here, we present a platform that fulfills the above criteria: it provides high transfection efficiency, proper targeting to the APCs, and an adjuvant effect. The platform is based on the synthesis, in a unique nanoparticle, of 2 technologies already independently tested with modest results: PADRE and PAMAM dendrimer.

The universal peptide PADRE binds/activates cells bearing any of the 15 major forms of the HLA-DR and has been widely used as immune adjuvant (14, 30, 31). Its adjuvant (although modest) effect has been confirmed in this report (Fig. 6A). In fact, coinjection of PADRE with unconjugated dendrimer loaded with TRP2-encoding plasmid marginally increased the efficacy of the vaccine. PAMAM dendrimers, because of their properties of DNA complexation and the capacity to be attached to the cell membrane, have been independently used as a platform for DNA vaccination (32) although only modest results were reported. Our data confirmed the capacity of unconjugated dendrimers to promote both humoral and cell-mediated immunity. Indeed, 4 of 5 mice immunized by unconjugated dendrimer show low affinity CTLs toward the antigen with which they were immunized (Fig. 4). This low immunity, however, is not sufficient to protect mice from the subsequent challenge with B16OVA or CT26 (Fig. 5) nor it is effective in therapeutic models (Figs. 6 and 7).

In striking contrast, the physical conjugation of the PAMAM dendrimer to the MHC class II-targeting peptide, dramatically increases the immunogenicity of the platform and the efficacy of DNA vaccines, overcoming the limitations of the current platform for DNA vaccination.

Both platforms presented here are able to preferentially deliver DNA to lymph nodal APCs where a selective transfection of DCs is observed (Fig. 3). This preferential transfection of professional APCs results in the induction of high affinity CTLs and of humoral response to the antigen delivered (Fig. 4). Interestingly, whereas PPD induces the appearance of a high number of transfected DC, a more limited number is found when HAPD is used (Fig. 3). Consistently IFN- γ secretion by CTLs in response to stimulation with the relevant tumor is lower when HAPD is used (Fig. 4). Although we cannot exclude that the reason for these different responses lies in the tumor/antigen used (TRP2 or AH1) or in intrinsic strain differences (C57BL/6 or BALB/c), it is possible that the adjuvant activity of PADRE plays a role.

As expected, PPD is the most promising of the 2 platforms described in this article: it not only generates high affinity memory CTLs and a strong humoral response but, in prevention models, it shows an efficacy far superior to that observed

with dermal electroporation. It is important to underline that dermal electroporation has been highly optimized with considerable industrial effort and investment and it is considered the gold standard for DNA vaccination by assuring: (i) high transfection efficiency, (ii) a danger signal, and (iii) and physical needle-mediated targeting of dermal APCs. Thus, our observations that the not-yet fully optimized PPD platform can generate a protective immunity superior to the one obtained with dermax suggests a potentially very high impact for this technology (Fig. 5).

The promise of this platform is further elucidated in the therapeutic setting where the delivery of pcDNA3-TRP2 via PPD leads to B16 tumor regression and mice survival is roughly 50%. The observation that TRP2 vaccination using unmodified dendrimers is ineffective and that only a modest increase in survival is achieved when PADRE is mixed with the vaccine (Fig. 6), strongly suggest that PADRE, when it is conjugated to the dendrimers in the PPD formulation, not only exerts an adjuvant effect (30, 31), but also can target the dendrimer and its DNA cargo to the appropriate APCs.

Considering that PADRE binds most human HLA-DR as well as monkey MHC class II (data not shown), the data presented here not only represents proof of concept of this new nanoparticle-based DNA vaccination but also suggests that PPD is a good candidate for DNA-based immunization in human diseases.

Disclosure of Potential Conflicts of Interest

P. Daftarian, B.B. Blomberg, V. Lemmon, A.E. Kaifer, W. Li, R. Chowdhury, V. Perez, and P. Serafini are named inventors on a patent application (filed by the University of Miami) on technologies described in this article and have potential financial benefits for its commercialization. Conflict of interest is managed by University of Miami. No potential conflicts of interest were disclosed by the other authors.

Acknowledgments

The authors thank D. Lopez, E. Podack, and V. Bronte for critically reading the manuscript.

Grant Support

This work was supported by the Sylvester Cancer Center, the Coulter Center, and the Susan Komen for the cure foundation award number KG090350.

The costs of publication of this article were defrayed in part by the payment of page charges. This article must therefore be hereby marked *advertisement* in accordance with 18 U.S.C. Section 1734 solely to indicate this fact.

Received May 23, 2011; revised September 21, 2011; accepted September 30, 2011; published OnlineFirst October 10, 2011.

References

- Widera G, Austin M, Rabussay D, Goldbeck C, Barnett SW, Chen M, et al. Increased DNA vaccine delivery and immunogenicity by electroporation *in vivo*. *J Immunol* 2000;164:4635-40.
- Cappelletti M, Zampaglione I, Rizzuto G, Ciliberto G, La Monica N, Fattori E. Gene electro-transfer improves transduction by modifying the fate of intramuscular DNA. *J Gene Med* 2003;5:324-32.
- Mennuni C, Calvaruso F, Facciabene A, Aurisicchio L, Storto M, Scarselli E, et al. Efficient induction of T-cell responses to carcinoem-bryonic antigen by a heterologous prime-boost regimen using DNA and adenovirus vectors carrying a codon usage optimized cDNA. *Int J Cancer* 2005;117:444-55.
- Rice J, Dossett ML, Ohlén C, Buchan SL, Kendall TJ, Dunn SN, et al. DNA fusion gene vaccination mobilizes effective anti-leukemic cytotoxic T lymphocytes from a tolerized repertoire. *Eur J Immunol* 2008;38:2118-30.
- Liu MA. Immunologic basis of vaccine vectors. *Immunity* 2010;33:504-15.

6. Leroux-Roels G. Unmet needs in modern vaccinology: adjuvants to improve the immune response. *Vaccine* 2010;28 Suppl 3:C25-36.
7. Pietersz GA, Tang CK, Apostolopoulos V. Structure and design of polycationic carriers for gene delivery. *Mini Rev Med Chem* 2006; 6:1285-98.
8. Tekade RK, Kumar PV, Jain NK. Dendrimers in oncology: an expanding horizon. *Chem Rev* 2009;109:49-87.
9. Agadjanyan MG, Ghochikyan A, Petrushina I, Vasilevko V, Movsesyan N, Mkrtichyan M, et al. Prototype Alzheimer's disease vaccine using the immunodominant B cell epitope from beta-amyloid and promiscuous T cell epitope pan HLA DR-binding peptide. *J Immunol* 2005;174:1580-6.
10. Velappan N, Clements J, Kiss C, Valero-Aracama R, Pavlik P, Bradbury AR. Fluorescence linked immunosorbant assays using microtiter plates. *J Immunol Methods* 2008;336:135-41.
11. De Palma R, Marigo I, Del Galdo F, De Santo C, Serafini P, Cingarlini S, et al. Therapeutic effectiveness of recombinant cancer vaccines is associated with a prevalent T-cell receptor alpha usage by melanoma-specific CD8+ T lymphocytes. *Cancer Res* 2004;64:8068-76.
12. Bronte V, Cingarlini S, Apolloni E, Serafini P, Marigo I, De Santo C, et al. Effective genetic vaccination with a widely shared endogenous retroviral tumor antigen requires CD40 stimulation during tumor rejection phase. *J Immunol* 2003;171:6396-405.
13. Rabussay D. Applicator and electrode design for *in vivo* DNA delivery by electroporation. *Methods Mol Biol* 2008;423:35-59.
14. Alexander J, Fikes J, Hoffman S, Franke E, Sacci J, Appella E, et al. The optimization of helper T lymphocyte (HTL) function in vaccine development. *Immunol Res* 1998;18:79-92.
15. Kim D, Monie A, He L, Tsai YC, Hung CF, Wu TC. Role of IL-2 secreted by PADRE-specific CD4+ T cells in enhancing E7-specific CD8+ T-cell immune responses. *Gene Ther* 2008;15:677-87.
16. Alexander J, Sidney J, Southwood S, Ruppert J, Oseroff C, Maewal A, et al. Development of high potency universal DR-restricted helper epitopes by modification of high affinity DR-blocking peptides. *Immunity* 1994;1:751-61.
17. Bloom MB, Perry-Lalley D, Robbins PF, Li Y, el-Gamil M, Rosenberg SA, et al. Identification of tyrosinase-related protein 2 as a tumor rejection antigen for the B16 melanoma. *J Exp Med* 1997;185: 453-9.
18. Bronte V, Apolloni E, Ronca R, Zamboni P, Overwijk WW, Surman DR, et al. Genetic vaccination with "self" tyrosinase-related protein 2 causes melanoma eradication but not vitiligo. *Cancer Res* 2000; 60:253-8.
19. Huang AY, Gulden PH, Woods AS, Thomas MC, Tong CD, Wang W, et al. The immunodominant major histocompatibility complex class I-restricted antigen of a murine colon tumor derives from an endogenous retroviral gene product. *Proc Natl Acad Sci U S A* 1996; 93:9730-5.
20. Roos AK, Eriksson F, Timmons JA, Gerhardt J, Nyman U, Gudmundsdottir L, et al. Skin electroporation: effects on transgene expression, DNA persistence and local tissue environment. *PLoS One* 2009;4: e7226.
21. Brumeanu TD, Casares S, Bot A, Bot S, Bona CA. Immunogenicity of a contiguous T-B synthetic epitope of the A/PR/8/34 influenza virus. *J Virol* 1997;71:5473-80.
22. Cursiefen C. Immune privilege and angiogenic privilege of the cornea. *Chem Immunol Allergy* 2007;92:50-7.
23. Hung CF, Yang M, Wu TC. Modifying professional antigen-presenting cells to enhance DNA vaccine potency. *Methods Mol Med* 2006; 127:199-220.
24. Jerome V, Graser A, Muller R, Kontermann RE, Konur A. Cytotoxic T lymphocytes responding to low dose TRP2 antigen are induced against B16 melanoma by liposome-encapsulated TRP2 peptide and CpG DNA adjuvant. *J Immunother* 2006;29:294-305.
25. Cohen AD, Diab A, Perales MA, Wolchok JD, Rizzuto G, Merghoub T, et al. Agonist anti-GITR antibody enhances vaccine-induced CD8(+) T-cell responses and tumor immunity. *Cancer Res* 2006;66:4904-12.
26. Nanni P, De Giovanni C, Lollini PL, Nicoletti G, Prodi G. TS/A: a new metastasizing cell line from a BALB/c spontaneous mammary adenocarcinoma. *Clin Exp Metastasis* 1983;1:373-80.
27. Gri G, Chiodoni C, Gallo E, Stoppacciaro A, Liew FY, Colombo MP. Antitumor effect of interleukin (IL)-12 in the absence of endogenous IFN-gamma: a role for intrinsic tumor immunogenicity and IL-15. *Cancer Res* 2002;62:4390-7.
28. Piconese S, Valzasina B, Colombo MP. OX40 triggering blocks suppression by regulatory T cells and facilitates tumor rejection. *J Exp Med* 2008;205:825-39.
29. Frelin L, Brass A, Ahlen G, Brenndorfer ED, Chen M, Sallberg M. Electroporation: a promising method for the nonviral delivery of DNA vaccines in humans? *Drug News Perspect* 2010;23:647-53.
30. Wu CY, Monie A, Pang X, Hung CF, Wu TC. Improving therapeutic HPV peptide-based vaccine potency by enhancing CD4+ T help and dendritic cell activation. *J Biomed Sci* 2010;17:88.
31. Kim D, Monie A, Tsai YC, He L, Wang MC, Hung CF, et al. Enhancement of CD4+ T-cell help reverses the doxorubicin-induced suppression of antigen-specific immune responses in vaccinated mice. *Gene Ther* 2008;15:1176-83.
32. Heegaard PM, Boas U, Sorensen NS. Dendrimers for vaccine and immunostimulatory uses. A review. *Bioconjug Chem* 2010;21: 405-18.

Cancer Research

The Journal of Cancer Research (1916–1930) | The American Journal of Cancer (1931–1940)

Peptide-Conjugated PAMAM Dendrimer as a Universal DNA Vaccine Platform to Target Antigen-Presenting Cells

Pirouz Daftarian, Angel E. Kaifer, Wei Li, et al.

Cancer Res 2011;71:7452-7462. Published OnlineFirst October 10, 2011.

Updated version Access the most recent version of this article at:
doi:[10.1158/0008-5472.CAN-11-1766](https://doi.org/10.1158/0008-5472.CAN-11-1766)

Supplementary Material Access the most recent supplemental material at:
<http://cancerres.aacrjournals.org/content/suppl/2011/12/13/0008-5472.CAN-11-1766.DC1>

Cited articles This article cites 32 articles, 11 of which you can access for free at:
<http://cancerres.aacrjournals.org/content/71/24/7452.full.html#ref-list-1>

Citing articles This article has been cited by 2 HighWire-hosted articles. Access the articles at:
</content/71/24/7452.full.html#related-urls>

E-mail alerts [Sign up to receive free email-alerts](#) related to this article or journal.

Reprints and Subscriptions To order reprints of this article or to subscribe to the journal, contact the AACR Publications Department at pubs@aacr.org.

Permissions To request permission to re-use all or part of this article, contact the AACR Publications Department at permissions@aacr.org.